International Journal of Applied Engineering Research ISSN 0973-4562 Volume 12, Number 21 (2017) pp. 11511-11522

Nonlinear analysis of degenerated FGM shells

B. Amieur [a], M. Djermane [a], F. Hammadi [b]

[a] *Reliability of Materials and Structures Laboratory, University Of Bechar, Algeria.*
[b] *Laboratory of Mechanics: Modelling and experimentation L2ME, University of Bechar, Algeria.*

[1,2,3]*Orcid: 0000-0002-9032-5380, 0000-0003-1267-1787, 0000-0002-7504-4580*

Abstract

In this work we deal with nonlinear behavior of functionally graded material for cylindrical panel and spherical structure. The formulation chosen in this work is based on Von Karman theory for large transverse deflection with the layer-by-layer approach. The mechanical properties are assumed to vary continuously through thickness direction according to the volume fraction of the constituents by a simple power law distribution. The shell element developed is based on a nine nodes degenerated finite element formulation with height order shear deformation theory. The effect of variations of volume fractions and shell geometrical parameters are studied, the influence of elastoplasticity is also the subject of this work. Convergence tests and comparison studies have been carried out to establish the efficiency of the present model.

Keywords: Composite, nonlinear, FGM, DDSE

INTRODUCTION

Because of their strength to weight ratio, high rigidity, long life of fatigue, resistance to electrochemical corrosion and other superior properties of composite materials, laminates have been used increasingly in variety industrial areas.

The design of the structures with better thermal and mechanical properties in addition to high stiffness to weight ratios and strength to weight ratios can be obtained with adaptation of the laminated composite structures but because of the sharp change in these properties at the interface between two adjacent layers causes initiation to delamination which can be avoided if the different properties continuously vary across the thickness and thus the use of FGM can become an important problem for advanced structural applications.

Recently, functionally graded materials (FGM) materials, which are readily manufactured from a mixture of a metal and a ceramic characterized by a continuous change of mechanical properties in the direction of thickness, have emerged as a new class of materials.

In literature many researchers studied static, dynamic and nonlinear behavior for elastic FGM structures in the past few years, only some of them are cited in this paper:

For example in 2006, Ashraf and Zenkour [1] presented the static response for simply supported functionally graded rectangular plates subjected to a transverse uniform load. In 2009 M. Simsek presented a static analysis of a functionally graded simply-supported beam subjected to a uniformly distributed load by using Ritz method within the framework of Timoshenko and the higher order shear deformation beam theories [2] and the mechanical behavior of FGM plates under transverse load is given by Chi and Chung [3],[4].

the research were continuing to take into account the nonlinear problems as is presented by Shen [5] when treated nonlinear bending analysis for a simply supported functionally graded rectangular plate subjected to transverse uniform load or sinusoidal load. In this studie the Galerkin technique is employed to determine load deflection and load bending deflection and load bending moments. A higher order theory for studying the bending response of functionally graded plates where the Von Karman theory is used for obtaining the approximate solutions for nonlinear bending is proposed by Lee et al. [6].

The temporal problems were the subject of several studies, including that of Amini et al. [7] which is summarized in the analysis of the free vibration of FGM plates on elastic foundations using three-dimensional linear elasticity theory, Sundararajan et al. [8] investigated the nonlinear free flexural vibrations of FGM rectangular and skew plates in thermal environments, respectively. Pradyumna et al. [9] analyzed in 2008 the free vibration of functionally graded curved panels using a higher-order C^0 finite element formulation.

Then nonlinear vibrations and dynamic response were studied by Huang and Shen [10] .Natural frequencies, compressive buckling loads, buckling temperature and bending deflections and stresses of FGM sandwich plates based on sinusoidal shear deformation plate theory and the nonlinear dynamic response of sandwich plates resting on elastic foundations in thermal environments are analyzed and calculated by Zenkour [11]; Zenkour and Sobhy [12]; Zenkour and Alghamdi [13] and Zhen-Xin Wang et al. [14]. And Thermal post buckling and vibration behaviour of FGM plates were studied by Park and Kim [15].

In order to trace the equilibrium path beyond critical points, a more general incremental control strategy is needed, in which

displacement and load increments are controlled simultaneously. This strategy known by controlled arc length method was not used in the case of composite materials according to the literature to date, from this documents and researches also in my knowledge; the elastic-plastic analysis, which is also the subject of this work, is not treated in the FGM type case of composites materials only by Moita et all in 2016 [16].

EFFECTIVE MATERIAL PROPERTIES OF FGMS:

In the first we consider a simple square FGM plate as shown in the Fig.1.

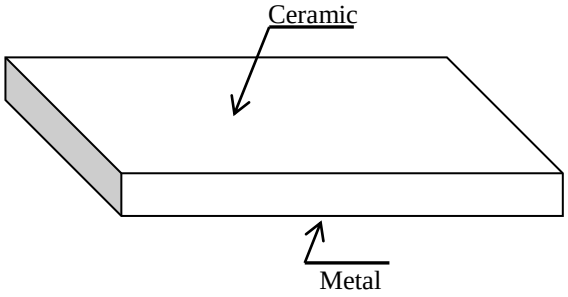

Figure 1: FGM plate.

The mechanical properties are determined according to the volume fraction when we consider that the plate is made up of a mixture of the ceramic as top face sheet and the metal as bottom face sheet as following[17][18]:

$$P(z) = P_c V_c + P_m V_m \qquad (1)$$

Where $P(z)$ is the effective properties which can be the Young modulus $E(z)$, the Poisson ratio $\nu(z)$, the yield stress $\sigma_Y(z)$ or the density $\rho(z)$, the thermal expansion coefficient $\alpha(z)$ or thermal conductivity $k(z)$.

V_m and V_c are the metal and ceramic volume fraction related by the relation:

$$V_m = 1 - V_c \qquad (2)$$

This allows rewriting [19]:

$$P(z) = (P_c - P_m)V_c + P_m \qquad (3)$$

Where Pm and Pc denotes the metal and ceramic properties and V_c denotes the volume fraction chosen according to the power low, segmoidal law or exponential law.

In the case of power law (P-FGM), the volume fraction is given by: $V_c = \left(\frac{1}{2} + \frac{z}{h}\right)^k$, in which $k \geq 0$ is a parameter that dictates the material variation profile through the thickness.

This expression can be written in curvilinear coordinates as:

$$V_c = \left(\frac{1}{2} + \frac{\zeta}{2}\right)^k = \left(\frac{\zeta + 1}{2}\right)^k \qquad (4)$$

In the case of sigmoid FGM structures (S-FGM), the volume fraction is given by:

$$\begin{aligned} V_1 &= 1 - \frac{1}{2}\left(1 - \frac{2z}{h}\right)^k \qquad 0 \leq z \leq \frac{h}{2} \\ V_2 &= \frac{1}{2}\left(1 + \frac{2z}{h}\right)^k \qquad -\frac{h}{2} \leq z \leq 0 \end{aligned} \qquad (5)$$

By using the rule of mixture, the material properties of the S-FGM can be calculated by:

$$\begin{aligned} &P(z) = (P_c - P_m)V_1 + P_m \qquad 0 \leq z \leq \frac{h}{2} \\ &And \qquad (6) \\ &P(z) = (P_c - P_m)V_2 + P_m \qquad -\frac{h}{2} \leq z \leq 0 \end{aligned}$$

The constitutive equation in elastic case is written as [20] [21]:

$$\begin{Bmatrix} \sigma_x \\ \sigma_y \\ \tau_{xy} \\ \tau_{xz} \\ \tau_{yz} \end{Bmatrix} = \begin{bmatrix} Q_{11} & Q_{21} & 0 & 0 & 0 \\ Q_{12} & Q_{22} & 0 & 0 & 0 \\ 0 & 0 & Q_{66} & 0 & 0 \\ 0 & 0 & 0 & Q_{44} & 0 \\ 0 & \circ & 0 & 0 & Q_{55} \end{bmatrix} \begin{Bmatrix} \varepsilon_x \\ \varepsilon_y \\ \gamma_{xy} \\ \gamma_{xz} \\ \gamma_{yz} \end{Bmatrix} = [D] \begin{Bmatrix} \varepsilon_x \\ \varepsilon_y \\ \gamma_{xy} \\ \gamma_{xz} \\ \gamma_{yz} \end{Bmatrix} \qquad (7)$$

With

$$Q_{11} = Q_{22} = \frac{E(z)}{1 - \nu^2} \ , \ Q_{12} = Q_{21} = \nu Q_{11} = \frac{\nu E(z)}{1 - \nu^2}$$

And $$Q_{44} = Q_{55} = Q_{66} = \frac{E(z)}{2(1 - \nu)}$$

In general case, the virtual strain is the sum of the virtual elastic strain and virtual plastic strain:

$$\{d\varepsilon\} = \{d\varepsilon^e\} + \{d\varepsilon^p\} = [D_{ep}]\{d\sigma\} \qquad (8)$$

Where the elastic part is given by the Hook low as:

$$\{d\varepsilon^e\} = [D]^{-1}\{d\sigma\}$$

And the plastic part is given by:

$$\{d\varepsilon^p\} = d\lambda \left\{\frac{\partial \phi}{\partial \sigma}\right\}$$

$d\lambda$ is called multiplier of plasticity and $\phi = \phi(\sigma, k)$ is the yield surface for which the differentiation is given by:

$$d\phi = \left\langle \frac{\partial \phi}{\partial \sigma} \right\rangle \{d\sigma\} + \left\langle \frac{\partial \phi}{\partial k} \right\rangle \{dk\}$$

On the flow surface, $d\phi$ vanishes which leads us to write:

$$\left\langle \frac{\partial \phi}{\partial \sigma} \right\rangle \{d\sigma\} = -\left\langle \frac{\partial \phi}{\partial k} \right\rangle \{dk\}$$

Introducing the strain hardening modulus $A = -\frac{1}{d\lambda}\left\langle \frac{\partial \phi}{\partial k} \right\rangle \{dk\}$, the elastoplastic constitutive matrix is given by: $\left[D_{ep}\right] = [D] - \frac{[D]\{a\}\{a\}^t [D]}{A + \{a\}^t [D]\{a\}}$ (9)

With $\{a\} = \left\{ \frac{\partial \phi}{\partial \sigma} \right\}$

THEORETICAL FORMULATION:

III.1. Displacement field

This formulation is based on the development of the finite element of degenerated shells of drilling type presented in an original manner in [22] and with modification in [23] and [24] [25] and for which the vector of displacements is given by:

$$\begin{Bmatrix} u \\ v \\ w \end{Bmatrix} = \sum N_i \begin{Bmatrix} u_i \\ v_i \\ w_i \end{Bmatrix}_{moy} + \frac{\zeta}{2} \sum t_i N_i \begin{Bmatrix} \tilde{v}_1^x, -\tilde{v}_2^x \\ \tilde{v}_1^y, -\tilde{v}_2^y \\ \tilde{v}_1^z, -\tilde{v}_2^z \end{Bmatrix} \begin{Bmatrix} \alpha_i \\ \beta_i \end{Bmatrix} \quad (10)$$

For Drilling Degenerated Shell Element (DDSE) presentation it is given by:

$$\begin{Bmatrix} u \\ v \\ w \end{Bmatrix} = \sum_i N_i \begin{Bmatrix} u_i \\ v_i \\ w_i \end{Bmatrix} + \frac{\zeta}{2} \sum_i t_i N_i \begin{bmatrix} 0 & n_{3i} & m_{3i} \\ -n_{3i} & 0 & l_{3i} \\ m_{3i} & -l_{3i} & 0 \end{bmatrix} \begin{Bmatrix} \alpha_i \\ \beta_i \\ \gamma_i \end{Bmatrix} \quad (11)$$

Where u_i, v_i and w_i are total displacements of the node i, while considering α_i, β_i and γ_i rotations of the nodal vectors related to the node i. l_{3i}, n_{3i} and m_{3i} are the cosine directors of the vector V_3^i who are normal on the mide surface. The shape functions for a Lagrangian 9 nodes element are given by:

$$N_i = \left[\frac{\xi_0}{2}(1+\xi_0) + (1-\xi^2)(1-\xi_i^2) \right] \left[\frac{\eta_0}{2}(1+\eta_0) + (1-\eta^2)(1-\eta_i^2) \right] \quad (12)$$

With $\xi_0 = \xi_i \xi$ and $\eta_0 = \eta_i \eta$

The principle of virtual works allows achieving the tangent matrix given as sum of a linear part, nonlinear and initial stresses matrix:

$$[K_t] = [K_l] + [K_{NL}] + [K_\sigma] \quad (13)$$

The linear part is given by:

$$[K_l] = \int_v [B]^T [D_{ep}][B] dV \quad (14)$$

The nonlinear part is given by:

$$[K_{nl}] = \int_v [B_{nl}]^T [D_{ep}][B_{nl}] dV \quad (15)$$

And the initial stresses matrix is given by:

$$[K_\sigma] = \int_v [G]^T [S][G] dV \quad (16)$$

Where $[S] = \begin{bmatrix} \sigma_x I_3 & \tau_{xy} I_3 & \tau_{xz} I_3 \\ & \sigma_y I_3 & \tau_{yz} I_3 \\ & & \sigma_z I_3 \end{bmatrix}$

I_3 represents 3 x 3 identity matrix.

$[B]$ and $[B_{nl}]$ are the matrix linking stress to the nodal displacements which are obtained from Green-Lagrange field in general case.

$$\begin{Bmatrix} \varepsilon_x \\ \varepsilon_y \\ \varepsilon_z \\ \gamma_{xy} \\ \gamma_{yz} \\ \gamma_{xz} \end{Bmatrix} = \begin{Bmatrix} U_{,x} \\ V_{,y} \\ W_{,z} \\ U_{,y} + V_{,x} \\ V_{,z} + W_{,y} \\ U_z + W_{,x} \end{Bmatrix} + \begin{Bmatrix} \frac{1}{2}\left(U_{,x}^2 + V_{,x}^2 + W_{,x}^2\right) \\ \frac{1}{2}\left(U_{,y}^2 + V_{,y}^2 + W_{,y}^2\right) \\ \frac{1}{2}\left(U_{,z}^2 + V_{,z}^2 + W_{,z}^2\right) \\ (U, xU, y+V, xV, y+W, xW, y) \\ (U, zU, y+V, zV, y+W, zW, y) \\ (U, xU, z+V, xV, z+W, xW, z) \end{Bmatrix} \quad (17)$$

The field of transverse shear deformation is given by substitution of development of relations [26]:

$$\begin{aligned} \bar{\gamma}_{\xi\zeta} &= b_1 + b_2\xi + b_3\eta + b_4\xi\eta + b_5\eta^2 + b_6\xi\eta^2 \\ \bar{\gamma}_{\eta\zeta} &= c_1 + c_2\xi + c_3\eta + c_4\xi\eta + c_5\xi^2 + c_6\xi^2\eta \end{aligned} \quad (18)$$

This transversal shear deformations field is chosen such that it checks out the continuity between and inter-element and, therefore decreasing polynomial's degree generate the appearance of spurious modes.

These fields are also given by:

$$\begin{aligned} \bar{\gamma}_{\xi\zeta} &= \sum_{i=1}^{3}\sum_{j=1}^{2} Q_i(\eta)\overline{Q}_j(\xi)\gamma_{\xi\zeta}^{ij} \\ \bar{\gamma}_{\xi\zeta} &= \sum_{i=1}^{3}\sum_{j=1}^{2} Q_i(\xi)\overline{Q}_j(\eta)\gamma_{\eta\zeta}^{ij} \end{aligned} \quad (19)$$

With

$$\begin{aligned} Q_1(z) &= \frac{z}{2b}\left(\frac{z}{b}+1\right);\ Q_2(z) = 1 - \left(\frac{z}{b}\right)^2 \\ Q_3(z) &= \frac{z}{2b}\left(\frac{z}{b}-1\right) \\ \overline{Q}_1(z) &= \frac{1}{2}\left(\frac{z}{b}+1\right);\ \overline{Q}_2(z) = -\frac{1}{2}\left(\frac{z}{b}-1\right) \end{aligned} \quad (20)$$

Where b is the half of the plate dimension in the ξ *and* η directions.

NUMERICAL EXAMPLES

In this section, various analysis are performed by different authors [27],[28],[29] and [30] for the sandwich plates and the cylindrical panels and quadratic shell in the static linear and nonlinear cases with isotropic case and laminates or FGM for composites materials case to test various problems, by taking into account geometrical and material non linearity.

Static nonlinear cylindrical panel

As shown in Fig.2., we consider a cylindrical panel with length of 508 mm, radius of 254 mm and a thickness of 12.7 mm. The panel is subjected to a point load in the center. Because of the symmetry only a quarter of the structure is discretized into 2x2, 4x4 and 5x5, 9 nodes finite elements.

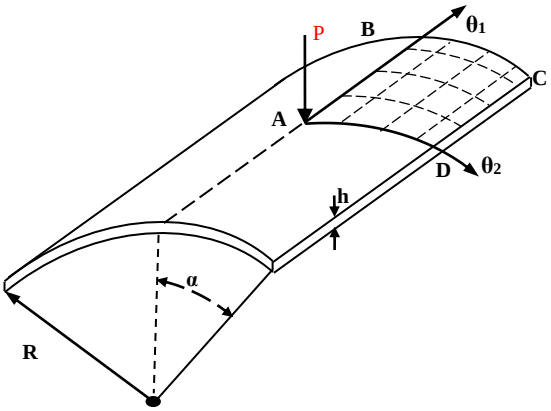

Figure 2:. FGM Cylindrical panel

The cylindrical panel is made of aluminium as the metal and ceramic such as zirconium with a continuous variation of properties according to the power distribution through the thickness.

For this example an isotropic material, laminated material and a FGM composite type were used in order to compare the behaviour of the panel in every one of these cases.

For FGM case:

$E_m = 70\,Gpa, \sigma_Y = 40$ Mpa and $\nu = 0.3$

$E_c = 151\,Gpa, \sigma_Y = 240$ Mpa and $\nu = 0.3$

Solving this problem with the following boundary conditions:

$u = v = w = \theta_x = 0$ along the side DC

And the symmetric conditions:

$u = \theta_y = 0$ along the side AB.

$v = \theta_x = 0$ along the side AD.

Leads us to the results showed in Figures:

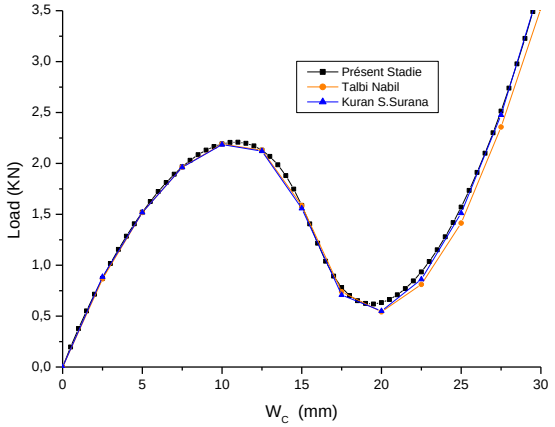

Figure 3.a. Deflection at the center for isotropic case.

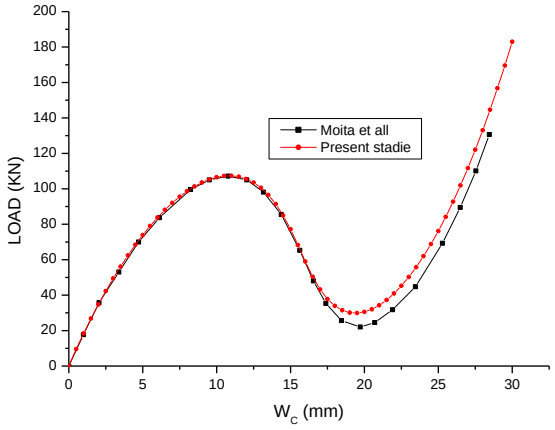

Figure 3.b. Deflection at the center for FGM case.

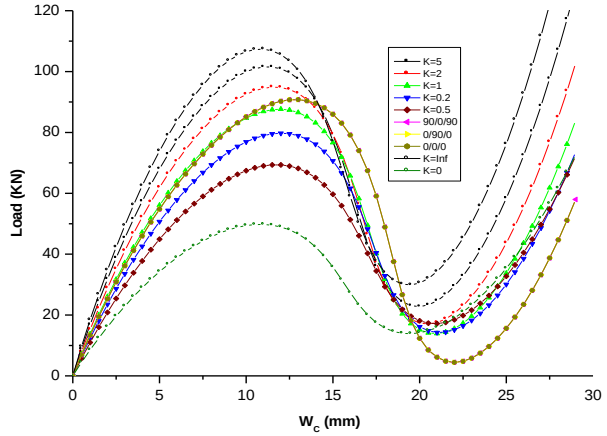

Figure 4: Deflection at the center for continuous and discontinuous variation of properties through the thickness.

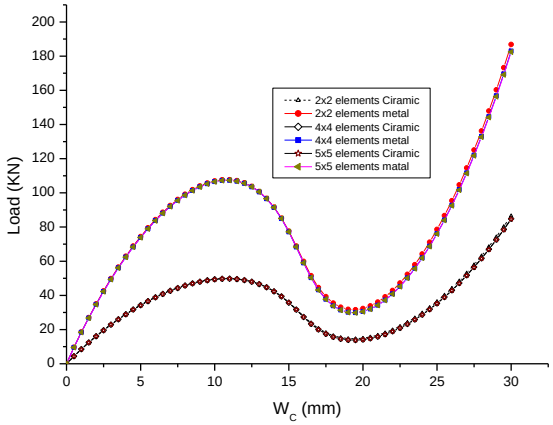

Figure 5.a: Effect of elements number on the deflection

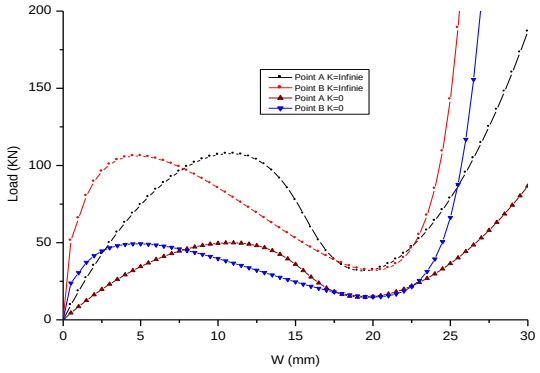

Figure 5.b: deflection at 2 distant points

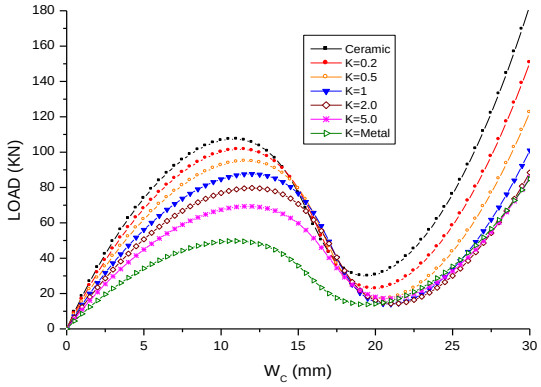

Figure 5.c: Effect of the volume fraction index on the deflection at point A

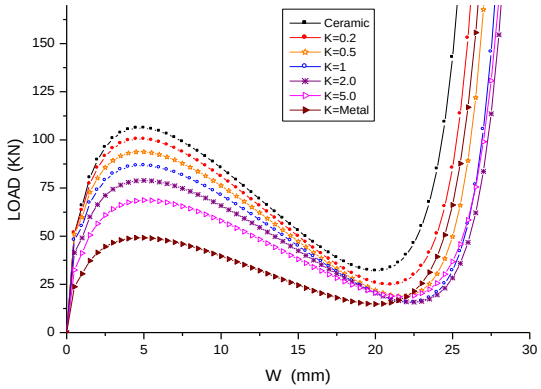

Figure 5.d: Effect of the volume fraction index on the deflection for 2x2 elements at point B

Figure 3.a represents deflection at the center of the cylindrical panel in the isotropic case with mechanical properties $E = 3.10275\, KN/mm^2$; $\upsilon = 0.3$ where it is clearly shown that the present work is confused with those of Talbi Nabil and Kuran S. Suranna [31], figure 3.b shows the good agreement between the result of the present study and its of Moita et all [16] in the FGM panel case.

In figure 4 we represent the variation of the center deflection of the cylindrical panel for the laminate case 90/0/90 and 0/90/0, and for varying values of volume fraction index k of an FG material, where the imposed displacement technique is used in the geometric nonlinearity case.

We note that the curves for the 0/90/0 and 90/0/90 laminated case are confused because there is no variation in the material properties along the x and y axis.

Figure 5.b shows the variation of the deflection at different points in function of the load applied to the panel center (point

A), for different values of the volume fraction index k, with a thickness h = 12.7 mm for the case of an FGM material.

For different discretizations in figure 5.a, we note that the curves are combined, it is for this reason that we adopt subsequently the 2X2 mesh elements.

From the curves of Fig.5.c and Fig.5.d can be seen that by increasing of the volume fraction index k, the limit load increases. It can be seen also as more as we move away from the load's application point, the more the deflection decreases but the limit load remains the same.

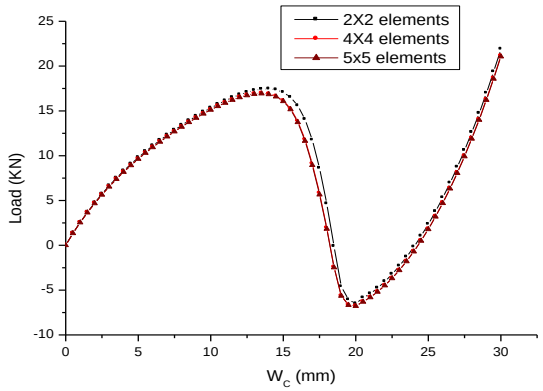

Figure 6.a: effect of elements number on the deflection for k=5

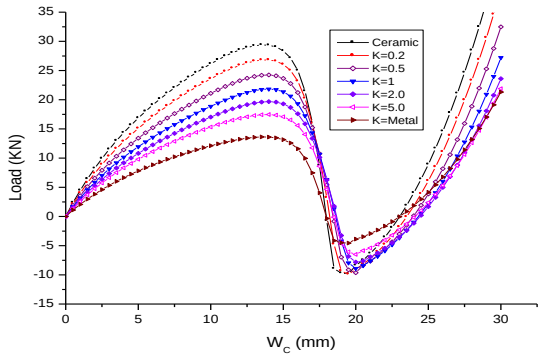

Figure 6.b: Effect of the volume fraction index on the deflection for 2x2 elements

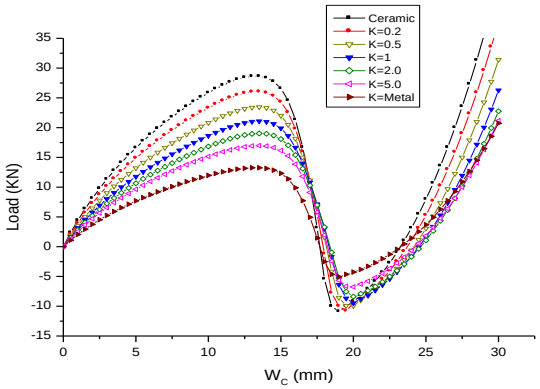

Figure 6.c: effect of the volume fraction index on the deflection for 4x4 elements

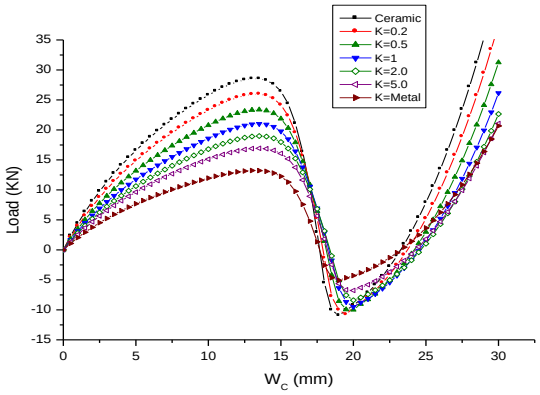

Figure 6.d: effect of the volume fraction index on the deflection for 5x5 elements

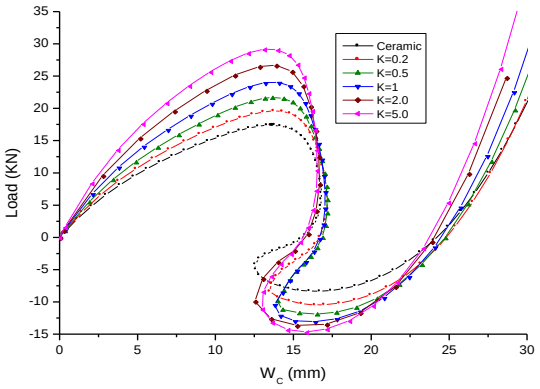

Figure 6.e: effect of the volume fraction index on the deflection using Arc length method.

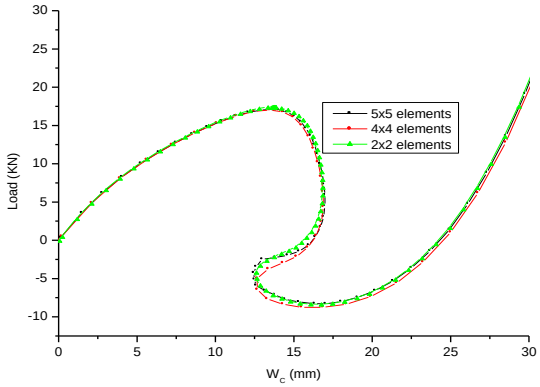

Figure 6.f: effect of the elements number on the deflection for k=5.

The 50% reduction in thickness, leads to a reduction of 75% of the limit load which can be seen in Fig.6.a

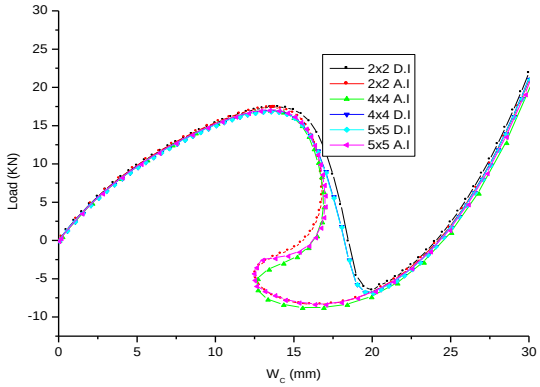

Figure 6.g: effect of the elements number for arc length and imposed displacement method on the deflection k=5.0

Figure 6.b, 6.c and 6.d represent the variation of the deflection depending on the load for a thickness h = 6.35 mm, with the use of the imposed displacement method that do not accurately reflect the geometrically nonlinear behaviour, which requires the use of the imposed arc length method because of the existence of a backspace.

On Fig.6.e and Fig.6.f we represent the deflection depending on the load for different values of the index of volume fraction using the imposed arc method which does not represent any difficulty.

On Fig.6.g we represent the difference between the use of the imposed displacement method and the imposed arc length method to better illustrate this numerical difference.

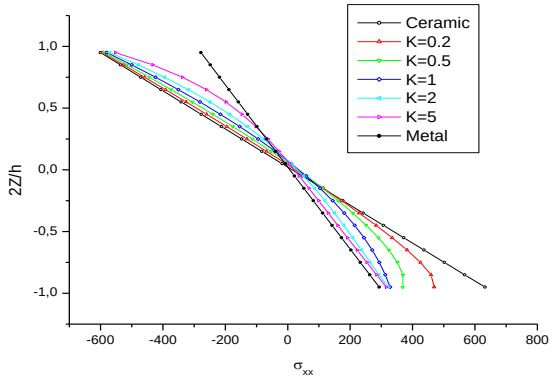

Figure 7.a: variation in the normal stress along y through the thickness.

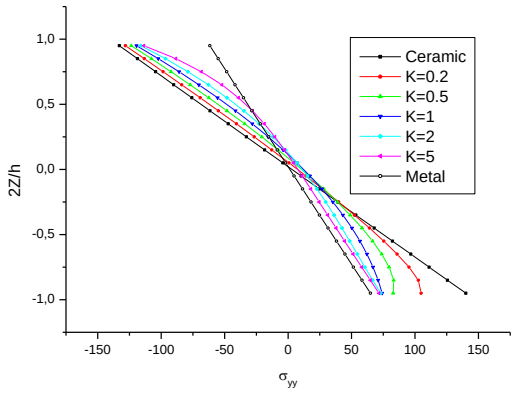

Figure 7.b: variation in normal stress along y through the thickness.

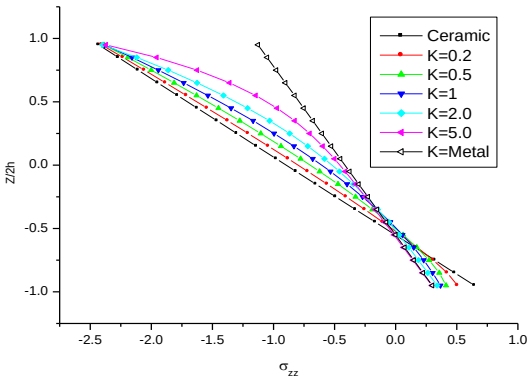

Figure 7.c: variation in normal stress along z through the thickness.

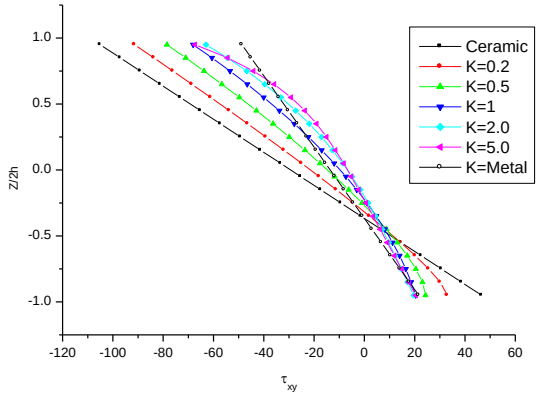

Figure 7.d: variation in tangential stress along y through the thickness.

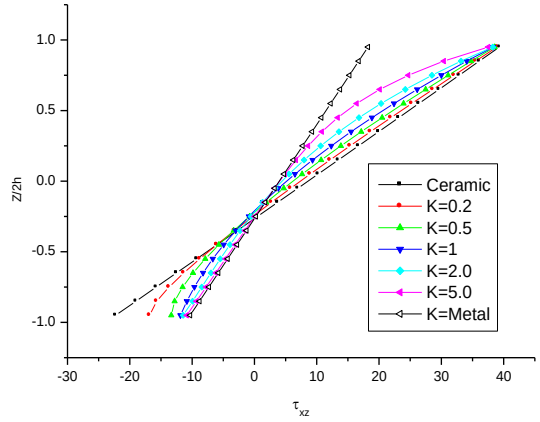

Figure 7.e: variation in tangential stress along y through the thickness.

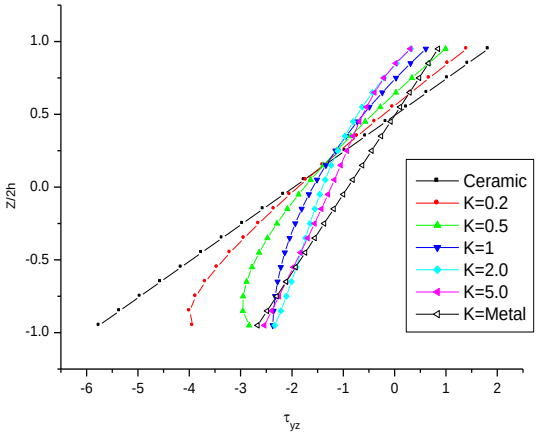

Figure 7.f: variation in tangential stress along y through the thickness.

Figure 7 shows the variation of normal and tangential stresses in the direction of thickness for different values of the index k for volume fraction of a thickness h = 12.7 mm at the end of the cycle non-linear. Firstly it should be noted that the stress σ_z, τ_{xz} and τ_{yz} as shown in Fig.7.c, Fig.7.e and Fig.7.f are negligible compared to the other stress which is justified by the theory of shells used.

In the case of a pure metal or pure ceramic, the normal stress σ_x and σ_y in Fig 6.a and Fig 6.b are linear and symmetrical, unlike in the cases where the material is a mixture between the ceramic and metal.

From the results obtained it can be seen the existence of the compression in ceramic zone and a traction in the metal fibers.

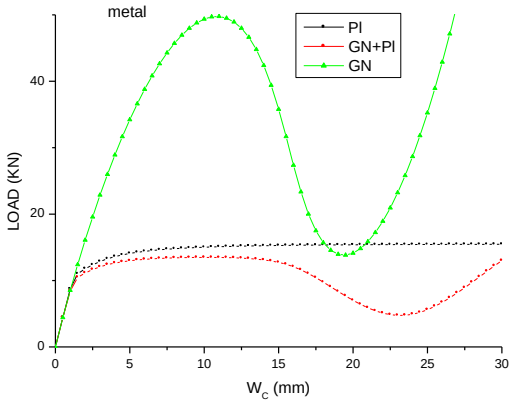

Figure 8.1: effect of elastic plastic on the geometric nonlinearity for metal.

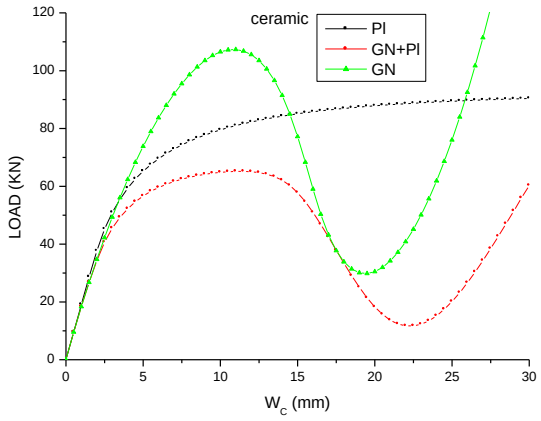

Figure 8.2: effect of elastic plastic on the geometric nonlinearity in the case of ceramic.

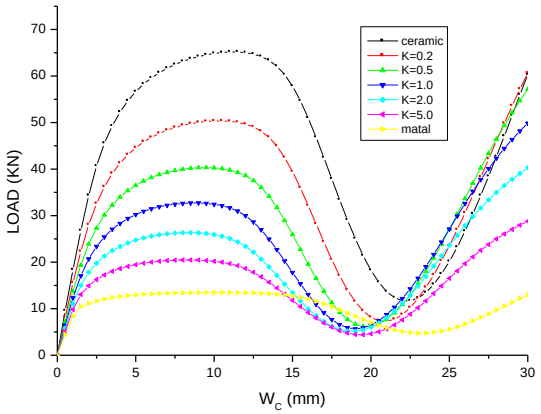

Figure.8.3: effect of elastic plastic on the geometric nonlinearity for different values of volume fraction index k.

In Fig 8.1 and Fig 8.2 we represent the load-displacement curve for the metal and ceramic for geometrically nonlinear (GN) combined with elastic plastic case (PL).

Fig.8.3, shows the load-displacement curve at the center of panel according to the volume fraction index, to see the effect of plasticity on the geometric nonlinearity, and from the result obtained it is clearly seen that this effect decreases with the decrease of k factor with the appearance of the limit point.

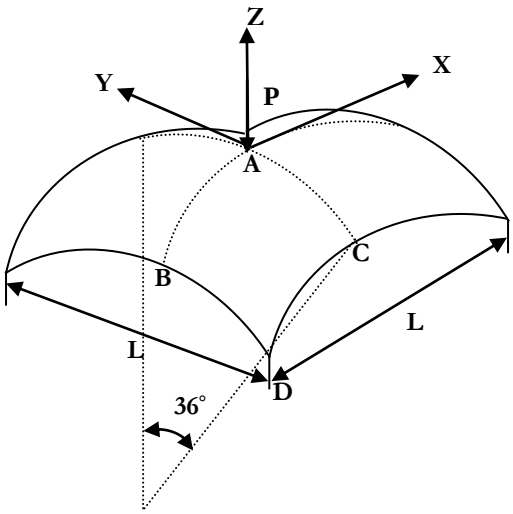

Figure 9: quadratic shell subjected to a concentrated load

Nonlinear quadratic shell with concentrated load

In this section the quadratic shell subjected to a concentrated load as shown in Fig.9. with thickness of 4 mm, all edges are clamped. The shell is made with two materials for which the properties used are:

$E_m = 70\,Gpa, \sigma_Y = 40$ Mpa and $\nu = 0.3$

$E_c = 151\,Gpa, \sigma_Y = 240$ Mpa and $\nu = 0.3$

Because of the symmetric of the structure, only the quarter is discritized to 3x3 elements with 9 nodes.

The aim of the analysis is to show the effect of the plasticity and geometrically nonlinearity on the structure when the properties change continuously by varying the volume fraction index from k=0 (pure ceramic case) to k=∞ (pure metal case).

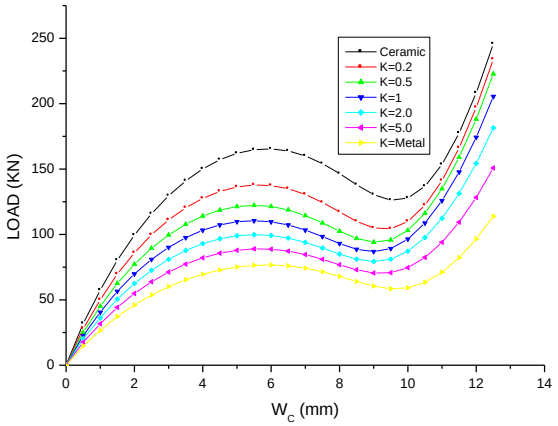

Figure 10.1: elastic deflection at the center for different values of volume fraction index k.

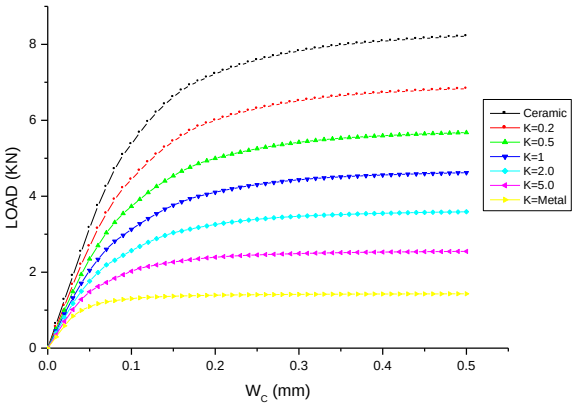

Figure 10.2: elastic plastic deflection at the center for different values of volume fraction index k.

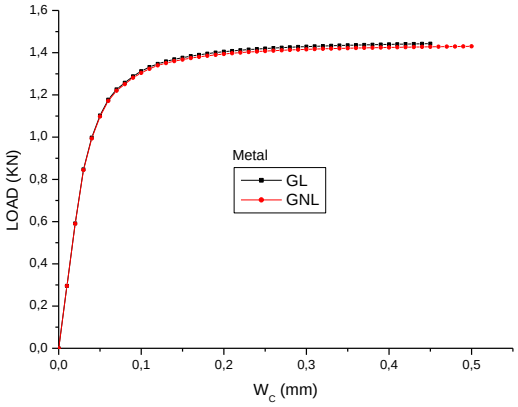

Figure 10.3: elastic and elastic plastic deflection at the center for the pure metal case.

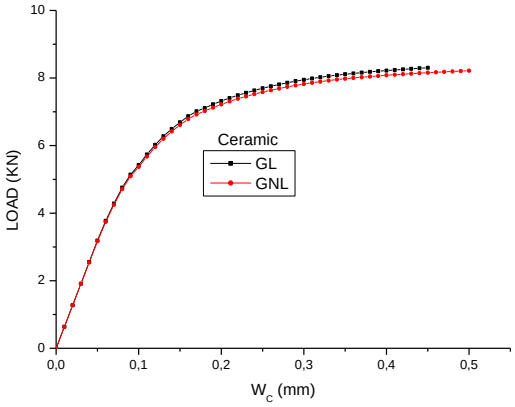

Figure 10.4: elastic and elastic plastic deflection at the center for the pure ceramic case.

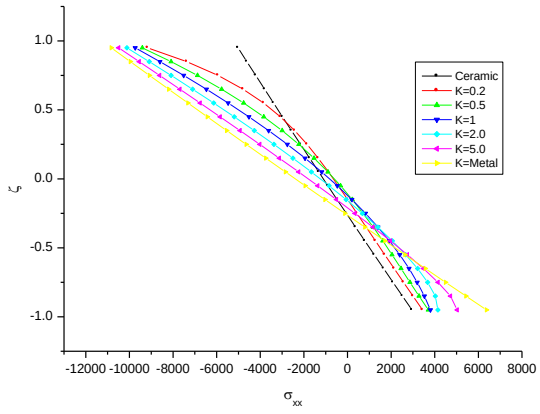

Figure 10.5: variation in the normal stress along y through the thickness.

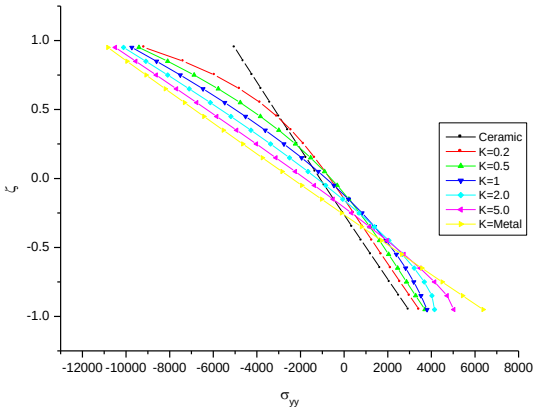

Figure 10.6: variation in the normal stress along y through the thickness.

In Fig 10.1, showing the elastic load-displacement curve, on which it is noticed that the value of the limit point decrease with increasing volume fraction index k. So the relationship limit point is proportional inversely to k and the displacement is directly proportional to k.

In Fig 10.2, we represent the load-displacement curve in the elastic and elastic-plastic geometrically nonlinear cases, we notices the disappearance of the limit point which means that the elastic-plastic is dominant in this case because the lamination is reached before the limit point.

In the fig 10.3 and Fig 10.4, a slight difference is noted in the case of elastic and elastic-plastic case for pure ceramic and pure metal.

We can also note the figures, Fig 10.5 and Fig 10.6 that because of the symmetry, the values of the normal stresses on x and y axis are equal.

These stresses are linear for pure ceramic case and the pure metal case but are nonlinear when the material is a composition between them.

In the elastic-plastic case, these stresses are nonlinear even in the pure metal case or pure ceramic case.

CONCLUSIONS

Linear and nonlinear static behavior of cylindrical shell panel and quadratic shell with Functionally Graded Material, in which the material proprieties vary through the thickness, have been presented for different values of volume fraction index in the case of a power law. The formulation is based on the Von Karman field for geometrically nonlinear. The central deflection, stress are analyzed for the panel and quadratic shell under a mechanical punctual load at the center.

These numerical results show also that it recommended using the controlled arc length method to give correctly the nonlinearity behaviour in the case of existence of a snap- back point.

REFERENCES

[1] Zenkour A.M., 2006. Generalized shear deformation theory for bending analysis of functionally graded plates. *Applied Mathematical Modeling*. Vol. 30, No. 1, pp. 67-84.

[2] M. Simsek, Static analysis of a functionally graded beam under a uniformly distributed load by Ritz method, International Journal of Engineering and Applied Sciences(IJEAS), Vol.1, Issue 3(2009)1-11.

[3] Chi SH, Chung YL. Mechanical behavior of functionally graded material plates under transverse load-Part I: Analysis. *Int J Solids Struct 2006*;43:3657–74.

[4] Chi SH, Chung YL. Mechanical behavior of functionally graded material plates under transverse load-part II: numerical results. *Int J Solids Struct 2006*;43:3675–91.

[5] Shen H.-S., 2002. Generalized shear deformation theory for bending analysis of functionally graded plates. *International Journal of Mechanical Sciences*, Vol. 44, No. 3, pp. 561-584.

[6] Lee K.H., Senthilnathan N.R, Lim S.P, and Chow S.T., 1989. Nonlinear bending response of functionally graded plates subjected to transverse loads and in thermal environments. *International Journal of Non-Linear Mechanics*. Vol. 24, No. 2, pp. 127-137.

[7] Amin MH, Soleimani M, Rastgoo A. Three-dimensional free vibration analysis of functionally graded material plates resting on an elastic foundation. *Smart Mater Struct 2009*;18:1–9.

[8] N. Sundararajan, T. Prakash, M. Ganapathi, Nonlinear free flexural vibrations of functionally graded rectangular and skew plates under thermal environments, *Finite Elements in Analysis and Design 42 (2005)* 152–168.

[9] S. Pradyumna, J.N. Bandyopadhyay, Free vibration analysis of functionally graded curved panels using a higher-order finite element formulation, *Journal of Sound and Vibration 318 (2008)* 176–192.

[10] X.L. Huang, H.-S. Shen, Nonlinear vibration and dynamic response of functionally graded plates in thermal environments, International Journal of Solids and Structures 41 (2004) 2403–2427.

[11] Zenkour A.M., 2005. A comprehensive analysis of functionally graded sandwich pates: part 1-Deflectiona and stresses, *International Journal of Solids and Structures*, Vol. 42, pp. 5224-5242.

[12] Zenkour, A.M.,Sobhy,M.,2010.Thermal buckling of various types of FGM sandwich plates.Compos.Struct.93,93–102.

[13] Zenkour, A.M.,Alghamdi, N.A.,2010.Bending analysis of functionally graded sandwich plates under the effect of mechanical and thermal loads. *Mech.Adv.Mater. Struct*.17,419–432.

[14] Zhen-Xin Wang, Hui-ShenShen, Non linear dynamic response of sandwich plates with FGM face sheets resting on elastic foundations in thermal environments, *Ocean Engineering 57 (2013)* 99–110

[15] J.S. Park, J.H. Kim, Thermal postbuckling and vibration analyses of functionally graded plates, *Journal of Sound and Vibration 289 (2006)* 77–93.

[16] J.S. Moita, A.L. Araujo, C.M Mota Soares, C.A. Mota Souares, J. Herskovits, Material and Geometric Nonlinear Analysis of Functionally Graded Plate-Shell Type Structures*, (2016), Appl Compos Mater.*

[17] J. Suresh Kumar1, B. Sidda Reddy2,*, C. Eswara Reddy3, K. Vijaya Kumar Reddy4, "Geometrically non linear analysis of functionally graded material plates using higher order theory", *International Journal of Engineering, Science and Technology*, Vol. 3, No. 1, 2011, pp. 279-288

[18] A.H. Sofiyev *, The vibration and stability behavior of freely supported FGM conical shells subjected to external pressure, *Composite Structures 89 (2009)* 356–366.

[19] Mohammad Talha, B.N.Singh, "Large amplitude free flexural vibration analysis of shear deformable FGM plates using non linear finite element method", *Finite element in analysis and design*, 47 pp.394-401, 2011.

[20] S.C. Pradhan, "Vibration suppression of FGM shells using embedded magnetostrictive layerss", *International Journal of Solids and Structures 42 (2005)* 2465–2488.

[21] A.K. Upadhyay, K.K. Shukla, "Geometrically nonlinear static and dynamic analysis of functionally graded skew plates", Commun Nonlinear Sci Numer Simulat, 2013.

[22] Kanok-Nukulchai W., "A simple and efficient finite element for general shell analysis" *Int. Journal. For. Num. methods. Engng*, 14, pp. 179-200, 1979.

[23] Djermane M., Chelghoum A., Amieur B. and Labbaci B., "The linear and nonlinear thin shell analysis using a mix finite element with drilling degrees of freedom" , Int*. J. Appl. Eng*, pp 217-236, 2006.

[24] Djermane M., "Analyse des coques minces par la méthode des éléments finis utilisation d'un élément tortionnel" ,*Master thesis USTHB Alger*, 1991.

[25] Djermane M., Chelghoum A., Amieur B. and Labbaci B., "Nonlinear Dynamic Analysis of Thin Shells Using a Finite Element With Drilling Degrees of Freedom" , *Int. J. Appl. Eng*, pp 97-108, 2007.

[26] Huang. H.C and Hinton.E, " A New nine nodes degenerated shell element with enhanced membrane and shear interpolation", *Int. Journal for numerical methods Eng*; 22, pp.73-92, 1986.

[27] H.T.Y.Yang, S.Saigal and D.G.Liaw. "Advances of thin shell finite elements and some applications – version I ", computer $ structures, vol 35 (4) pp.481-504, 1990

[28] Reddy, J. N., "Gemetrically non-linear transient analysis of laminated composite plates." *AIAA Jnl*, 42, pp.621-629, 1983.

[29] S.Swaddiwudhipony and Z.S.Liu: "Dynamic response of large strain elasto-plastic plate and shell structures", *Thin- Walled structures*, vol 26 (4) 223-239, 1996.

[30] Alireza Beheshti, Shojaa Ramezani, Nonlinear element analysis of functionally graded structures by enhanced assumed strain shell elements, Applied Mathematical Modelling, (2014).

[31] B. Amieur, M. Djermane, Analyse du comportement des coques géométriquement linéaire et non linéaire Par la méthode des elements finis utilisation d'un élément à champs de déformations augmenté, (2011), *Journal of Science Research N 2, Vol. 1, p3-8,Université de Béchar*

[32] X. Zhao, K.M. Liew, Geometrically nonlinear analysis of functionally graded shells (2009) Int J Mech Sci, 51, pp. 131-144